

# Analysis of strain localization by a damage front approach

Prabu MANOHARAN

Ecole Centrale Nantes

1, rue de Noël  
Nantes  
44300

Thesis Advisors

Prof. Nicolas Moës

Prof. Steven Le-Corre

May-2009

## ABSTRACT

Manufacturing is a controlled deformation and damaging of material to obtain to the desired shape and properties. Numerical optimization of manufacturing process is very essential to achieve better quality parts at reduced cost. However their application is limited due to associated complexities introduced due to geometry such as large deformation and physics such as strain localization and thermal effects. The present study is focused on the numerical strategies on stain localization of the material and limited to quasi static elastic cases. The Johnson-cook Viscoplastic model and Non-local strain gradient Model were analyzed in a 1D bar and a new approach using level set is proposed as an alternative. Robustness of the proposed approach is demonstrated by applying different Damage functions and Damage evolution law to fit the desired material behavior. Use of Level set gives greater control over the damage zone and is computationally effective.

## INDEX

1.0	INTRODUCTION.....	1
2.0	MATERIAL MODELS FOR STRAIN LOCALIZATION.....	2
2.1	Johnson Cook Visco-plasticity .....	2
2.2	Gradient damage Model.....	3
2.3	Computation of damage using level set.....	10
3.0	MODELLING PARAMETERS.....	16
3.1	Johnson Cook Visco-plasticity.....	16
3.2	Gradient damage Model.....	17
3.3	Level set approach.....	19
4.0	RESULTS AND DISCUSSION.....	21
4.1	Johnson Cook Visco-plasticity.....	21
4.2	Gradient damage Model.....	23
4.3	Computation of damage using level set.....	26
4.3.1	Analytical Solution.....	26
4.3.1.1	Influence of Damage evolution law.....	27
4.3.1.2	Influence of Damage function.....	31
4.3.2	Finite element Solution.....	32
5.0	CONCLUSION.....	35
6.0	REFERENCE.....	36

## 1.0 INTRODUCTION

Manufacturing is a controlled deformation and damaging of material to obtain to the desired shape and properties. To precisely get the desired output at any repeated number of time an extensive knowledge of the process and the material behavior is very essential. At present various manufacturing processes are carried out by trial and error. Such an experimental process leads to delay in processing the parts and expensive in cases of intricate components. Numerical optimization of manufacturing process is a natural choice in the present scenario considering the robustness of the technique in various applications. In the past several numerical tools were developed dedicated for this purpose resulting in reduced cost and process time of the product. But application of them to certain processes such as machining, forming and shearing are limited due to difficulties in simulating them due to complexities associated to geometry such as large deformation and physics such as strain localization and thermal effects [1].

As the material deforms under shear loading the micro cracks appear in a diffusive way and then they combine to form a macro crack at the later stage. During the failure process the strain and damage accumulates in a narrow region known as shear band [2, 3]. The length of the band increases until rupture during the fracture process. The present study is focused on the numerical strategies on strain localization of the material and limited to quasi static elastic cases.

The size of the resulting shear zone is not dependent on the structure and it depends on the heterogeneities of the material such a failure process leads to structural size effect during simulation. It has been experimentally proved and incorporated in several techniques. Hence during modeling the length scale of the material should be incorporated in the constitutive relations [4, 5].

In the local elastic damage models the accumulation of strain i.e. strain softening is represented by a set of internal variables which act on the decrease in stiffness of the material at the macroscopic level [6]. Damage occurs without the dissipation of energy and density of dissipated energy is finite at each material point since damage localizes in to a zero volume, the total energy dissipated to form a crack vanishes. This leads to instability known as spurious strain localization and mesh

dependency during finite element computations. To circumvent this problem various model have been introduced and still remains an active research field due to associated difficulties with each of them. In the study models which have found extensive applications such as Gradient damage model and Viscoplastic regularization have been analyzed. A new approach using the level set is proposed as an alternative to model strain localization have been proposed.

The models were applied to a 1D bar to check its efficiency for Mesh dependency and Strain softening. It is found that the proposed approach is advantageous both computational and physically replicates a sound model.

## 2.0 MATERIAL MODELS FOR STRAIN LOCALIZATION

### 2.1 Johnson Cook Visco-plasticity

Johnson cook viscoplastic model is widely used to study the localization in high strain rates. Umberglo et.al carried out the simulation of machining to test the influence of various material parameters and they have found the output exhibits significant influence on the process [7]. In the present study the model is applied to a 1D bar to check its efficiency for Mesh dependency and Strain softening.

The constitutive equation is represented by the following

$$\sigma_{eq} = (A + B\varepsilon^n) \left( 1 + C \ln \left( \frac{\dot{\varepsilon}}{\dot{\varepsilon}_o} \right) \right) (1 - \hat{\theta}^m) \quad (2.1.1)$$

Where A is the yield strength of the material (MPa), B is the hardening modulus of the material (MPa), C is the strain rate sensitivity coefficient, n is the hardening coefficient and m the thermal coefficient.

$$\hat{\theta}^m = \frac{T - T_t}{T_m - T_t}, \text{ where } T_m \text{ and } T_t \text{ are the melting and transition temperature of the}$$

material.

The equilibrium equation is given as

$$\nabla \cdot \boldsymbol{\sigma} = 0 \quad (2.1.2)$$

The structural equilibrium equation is solved along with the heat equation obtained by neglecting the diffusion of heat in the material and it is given as

$$\frac{\partial T}{\partial t} = \frac{\boldsymbol{\sigma} : \dot{\boldsymbol{\varepsilon}}^p}{\rho_h C_p} \quad (2.1.3)$$

Where  $\dot{\boldsymbol{\varepsilon}}^p$  is the plastic strain rate of the material,  $\rho_h$  is the density of the material and  $C_p$  is the heat carrying capacity of the material.

## 2.2 Gradient damage Model

For the linear elastic material behaviour the stress strain relation is given by

$$\boldsymbol{\sigma} = (1 - D)^4 \mathbf{H} : \boldsymbol{\varepsilon} \quad (2.2.1)$$

Where  $\boldsymbol{\sigma}$  is the Cauchy stress tensor,  $\boldsymbol{\varepsilon}$  the linear strain tensor and  ${}^4\mathbf{H}$  the fourth-order Hookean stiffness tensor.

With the equilibrium equation as

$$\nabla \cdot \boldsymbol{\sigma} = 0 \quad (2.2.2)$$

In continuum theory the damage evolution is considered as the dominant dissipative mechanism. The undamaged material is characterized by  $D=0$ , and the completely damaged being  $D=1$ . The intrinsic material damage evolves as the function of strain equivalent  $\varepsilon_{eq}(\boldsymbol{\varepsilon})$  and its evolution is given by the damage evolution law. The state of damage is governed by the history parameter  $\alpha$ , which represents the maximum damage the material has experienced  $D = D(\alpha)$  [6]. This evolution of damage based on the local value of strain equivalent leads to mesh dependency i.e., strain localisation. Later Bazant and Pijaudier-Cabot introduced the Non-locality into the constitutive relation to remove mesh dependency [8,9].

In the Non-local model the damage evolution is related to the non-local strain equivalent  $\bar{\varepsilon}_{eq}$  which is computed as the weighted average of the local strain equivalent at the given point  $x$  as

$$\bar{\varepsilon}_{eq} = \frac{1}{V} \int_V g(\xi) \varepsilon_{eq}(x + \xi) dV, \quad \text{with} \quad \frac{1}{V} \int_V g(\xi) dV = 1 \quad (2.2.3)$$

Where  $g(\xi)$  is the weight function and  $\xi$  denotes the relative position vector pointing to the infinitesimal volume  $dV$ .

The Non-local equivalent strain is obtained through the Kuhn-Tucker relation  $\bar{\varepsilon}_{eq} \geq 0$ .

$$\dot{\alpha} \geq 0, \quad \bar{\varepsilon}_{eq} - \alpha \leq 0, \quad \dot{\alpha} (\bar{\varepsilon}_{eq} - \alpha) = 0 \quad (2.2.4)$$

The gradient damage formulation is derived from the Non-local approach [10, 11]. The non-local equivalent strain is replaced by

$$\bar{\varepsilon}_{eq} = \varepsilon_{eq} + c \nabla^2 \varepsilon_{eq} \quad (2.2.5)$$

Where  $c = \frac{1}{2R^3} \int_0^R \rho^4 g(\rho) d\rho$ ,  $R$  is the radius of the averaging spherical volume

and the weight function is of form  $g(\xi) = g(\rho)$ .

This explicit relation (2.2.5) leads to  $C^1$  continuity requirements in Finite element analysis due to the dependency on the Laplacian of the local strain equivalent. It is avoided by implicit incorporation of the gradient term as given below. This enables a  $C^0$  continuous finite element interpolation.

$$\bar{\varepsilon}_{eq} + c \nabla^2 \bar{\varepsilon}_{eq} = \varepsilon_{eq} \quad (2.2.6)$$

This equation has to be satisfied in addition to the equilibrium equation. The parameter  $c$  limits the localisation zone i.e. acts as a control over the domain in which the non-local equivalent strain is computed. In order to solve (2.2.6) the boundary conditions concerning the non-local strain equivalent has to be specified. The most often used boundary condition is

$$\nabla \bar{\varepsilon}_{eq} \cdot n = 0 \quad (2.2.7)$$

Thus the problem can be stated as

Equilibrium equation:  $\nabla \cdot \boldsymbol{\sigma} = 0$

Stress-strain relation:  $\boldsymbol{\sigma} = (1 - D)^4 \mathbf{H} : \boldsymbol{\varepsilon}$

Strain equivalent Condition:  $\bar{\varepsilon}_{eq} + c \nabla^2 \bar{\varepsilon}_{eq} = \varepsilon_{eq}$

Boundary condition:  $\mathbf{u} = \mathbf{u}^*$ ,  $\boldsymbol{\sigma} \cdot \mathbf{n} = \mathbf{f}$ , &  $\nabla \bar{\varepsilon}_{eq} \cdot \mathbf{n} = 0$

Internal variable:  $\alpha(0) = \alpha_i$ ,  $\dot{\alpha} \geq 0$ ,  $\bar{\varepsilon}_{eq} - \alpha \leq 0$ ,  $\dot{\alpha}(\bar{\varepsilon}_{eq} - \alpha) = 0$

Where  $\alpha_i$  is the initial value of the internal variable  $\alpha$

Damage Evolution:  $D = D(\alpha)$

The damage evolution law can be chosen to fit the experiments. Some of the possible functions are as stated below.

Parabolic stress strain Curve:

$$D = \frac{\bar{\varepsilon}_{eq}}{\varepsilon_{cr}} \quad (2.2.8)$$

Bilinear Stress strain curve:

$$D = \frac{\varepsilon_{ult} (\bar{\varepsilon}_{eq} - \varepsilon_{cr})}{\bar{\varepsilon}_{eq} (\varepsilon_{ult} - \varepsilon_{cr})} \quad (2.2.9)$$

Exponential stress-stain curve:

$$D = 1 - \frac{\varepsilon_{cr}}{\bar{\varepsilon}_{eq}} \exp\left(-b(\bar{\varepsilon}_{eq} - \varepsilon_{cr})\right) \quad (2.2.10)$$

Where  $\varepsilon_{cr}$  and  $\varepsilon_{ult}$  are the critical and ultimate strain of the material.  $b$  is the parameter which sets the slope of the exponential curve after the peak. Figure.1



shows the corresponding curves using  $E = 15000\text{Mpa}$ ,  $\varepsilon_{cr} = 2.10^{-4}$ ,  $\varepsilon_{ult} = 10^{-3}$  and  $b = 1200$ .

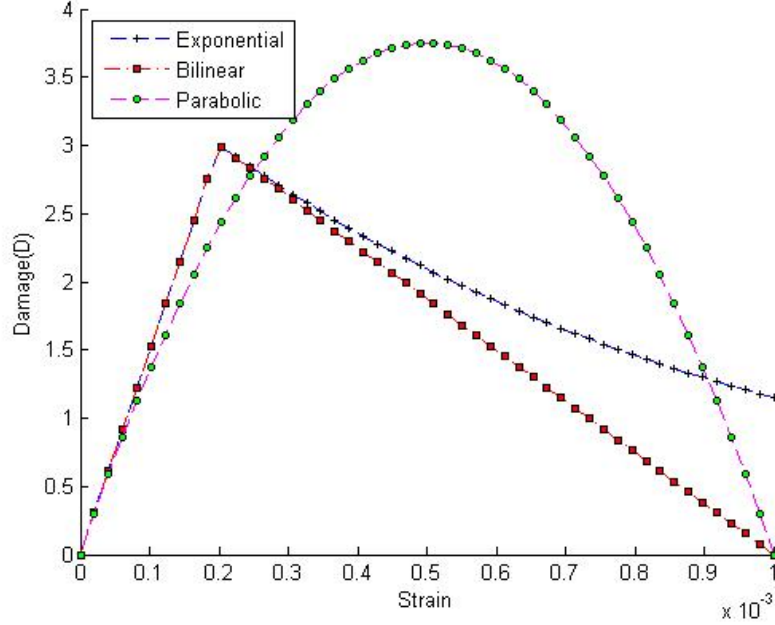


Figure1. Shows the damage evolution function used for the non-local gradient method.

Finite element Discretization of the equations is performed and the weak form of the equations is solved using the Newton Iterative solution procedure as detailed.

The weak form of the equation (2.2.2) is obtained by multiplying them with the weight function  $v(x)$  and by applying the divergence theorem.

$$\int_{\Omega} v \cdot (\nabla \cdot \boldsymbol{\sigma}) d\Omega = 0 \quad \forall v \in C^{-1} \quad (2.2.11)$$

$$\int_{\Omega} (\nabla v)^T \cdot \boldsymbol{\sigma} d\Omega = \int_{\Gamma} v \cdot p d\Gamma \quad \forall v \in C^0 \quad (2.2.12)$$

The weak form of the equation (2.2.6) is obtained by multiplying them with the weight function  $w(x)$ .

$$\int_{\Omega} w \left( \bar{\varepsilon}_{eq} + c \nabla^2 \bar{\varepsilon}_{eq} \right) d\Omega = \int_{\Omega} w \cdot \varepsilon_{eq} d\Omega \quad \forall w \in C^{-1} \quad (2.2.13)$$

and by applying the divergence theorem and the boundary condition for the strain equivalent

$$\int_{\Omega} (w \bar{\varepsilon}_{eq} + \nabla w c \nabla \bar{\varepsilon}_{eq}) d\Omega = \int_{\Omega} w \cdot \varepsilon_{eq} d\Omega \quad \forall w \in C^0 \quad (2.2.14)$$

Using the Galerkin approach the displacement and the weight functions are discretized using the same shape functions

$$u = \mathbf{N}u \quad (2.2.15)$$

$$v = \mathbf{N}v \quad (2.2.16)$$

The strain tensor components are given by the linear combination of the nodal displacement components

$$\varepsilon = \mathbf{B}u \quad (2.2.17)$$

$$\nabla v = \mathbf{B}v \quad (2.2.18)$$

Thus the equilibrium equation is discretized as shown below

$$\Rightarrow v^T \int_{\Omega} \mathbf{B}^T \boldsymbol{\sigma} d\Omega = v^T \int_{\Gamma} \mathbf{N}^T p d\Gamma \quad \forall v \quad (2.2.19)$$

Where  $p$  is the external force vector. The external and internal nodal forces are found as

$$f_{ext}^u = \int_{\Gamma} \mathbf{N}^T p d\Gamma \quad (2.2.20)$$

$$f_{int}^u = \int_{\Omega} \mathbf{B}^T \boldsymbol{\sigma} d\Omega \quad (2.2.21)$$

$$f_{int}^u = f_{ext}^u \quad (2.2.22)$$

The weak form of the equation (2.2.14) is discretized similarly using another interpolation function  $\mathbf{N}^e$  as below,

$$\bar{\varepsilon}_{eq} = \mathbf{N}^e \cdot \bar{\mathcal{E}}_{eq} \quad (2.2.23)$$

$$w = \mathbf{N}^e \cdot w \quad (2.2.24)$$

Using the derivatives of the shape functions the derivatives of non-local strain and its weight function is given as

$$\nabla \bar{\varepsilon}_{eq} = \mathbf{B}^e \cdot \bar{\mathcal{E}}_{eq} \quad (2.2.25)$$

$$\nabla w = \mathbf{B}^e \cdot w \quad (2.2.26)$$

Thus the discretized form of the average non-local strain equivalent equation is written as

$$w^T \int_{\Omega} (\mathbf{N}^{eT} \mathbf{N}^e + \mathbf{B}^{eT} \mathbf{B}^e) \bar{\boldsymbol{\varepsilon}}_{eq} d\Omega = w^T \int_{\Omega} \mathbf{N}^{eT} \boldsymbol{\varepsilon}_{eq} d\Omega \quad \forall w \quad (2.2.27)$$

And it is represented as

$$\mathbf{K}^{\varepsilon\varepsilon} \bar{\boldsymbol{\varepsilon}}_{eq} = \mathbf{f}^{\varepsilon} \quad (2.2.28)$$

In which

$$\mathbf{K}^{\varepsilon\varepsilon} = \int_{\Omega} (\mathbf{N}^{eT} \mathbf{N}^e + \mathbf{B}^{eT} \mathbf{B}^e) d\Omega \quad (2.2.29)$$

$$\mathbf{f}^{\varepsilon} = \int_{\Omega} \mathbf{N}^{eT} \boldsymbol{\varepsilon}_{eq} d\Omega \quad (2.2.30)$$

In the equilibrium equation the non-linearity is introduced by the damage relation. This Material non-linearity is solved by using Newton-Raphson iterative procedure to get approximation of the solution. Linearization of the stress-strain relation leads to

$$\boldsymbol{\delta}\boldsymbol{\sigma}_i = (1 - D_{i-1}) \mathbf{H} \boldsymbol{\delta}\boldsymbol{\varepsilon}_i - \delta D_i \mathbf{H} \boldsymbol{\varepsilon}_{i-1} \quad (2.2.31)$$

Where  $i$  and  $i-1$  denotes the current and previous iterative values.

For the derivatives of shape functions the change in strain field is written as

$$\boldsymbol{\delta}\boldsymbol{\varepsilon}_i = \mathbf{B} \boldsymbol{\delta}\mathbf{u}_i \quad (2.2.32)$$

For the damage loading the internal variable is to satisfy

$$\alpha = \bar{\boldsymbol{\varepsilon}}_{eq} \Rightarrow \delta\alpha_i = \delta\boldsymbol{\varepsilon}_{eq,i} \quad (2.2.33)$$

When there is no increase in damage  $\delta\alpha_i = 0$

Damage evolution is taken care by comparing the value of the converged non-local equivalent strain to the history value of the internal variable. The change in damage is given as

$$\delta D_i = q_{i-1} \mathbf{N}^e \boldsymbol{\delta}\bar{\boldsymbol{\varepsilon}}_{eq,i} \quad (2.2.34)$$

Where

$$q_{i-1} = \begin{cases} \left( \frac{\partial D}{\partial \alpha} \right)_{i-1} & \text{if } \bar{\varepsilon}_{eq,i-1} > \alpha_o \\ 0 & \text{if } \bar{\varepsilon}_{eq,i-1} \leq \alpha_o \end{cases} \quad (2.2.35)$$

Thus the linearized stress equation is written as

$$\Rightarrow \delta \boldsymbol{\sigma}_i = (1 - D_{i-1}) \mathbf{H} \mathbf{B} \delta u_i - \mathbf{H} \boldsymbol{\varepsilon}_{i-1} q_{i-1} \mathbf{N}^e \delta \bar{\boldsymbol{\varepsilon}}_{eq,i} \quad (2.2.36)$$

Using (2.2.36) the iterative change of internal force vector is written as

$$\delta f_{int,i}^u = \int_{\Omega} \mathbf{B}^T (1 - D_{i-1}) \mathbf{H} \mathbf{B} d\Omega \delta u_i - \int_{\Omega} \mathbf{B}^T \mathbf{H} \boldsymbol{\varepsilon}_{i-1} q_{i-1} \mathbf{N}^e d\Omega \delta \bar{\boldsymbol{\varepsilon}}_{eq,i} \quad (2.2.37)$$

$$\mathbf{K}_{i-1}^{uu} \delta u_i + \mathbf{K}_{i-1}^{ue} \delta \bar{\boldsymbol{\varepsilon}}_{eq,i} = f_{ext}^u - f_{int,i-1}^u \quad (2.2.38)$$

With

$$\mathbf{K}_{i-1}^{uu} = \int_{\Omega} \mathbf{B}^T (1 - D_{i-1}) \mathbf{H} \mathbf{B} d\Omega \quad (2.2.39)$$

$$\mathbf{K}_{i-1}^{ue} = - \int_{\Omega} \mathbf{B}^T \mathbf{H} \boldsymbol{\varepsilon}_{i-1} q_{i-1} \mathbf{N}^e d\Omega \quad (2.2.40)$$

Similarly the non-local strain equivalent equation is linearized as below

$$\delta \boldsymbol{\varepsilon}_{eq,i} = \mathbf{B} \delta u_i \quad (2.2.41)$$

$$\mathbf{K}_{i-1}^{eu} \delta u_i + \mathbf{K}_{i-1}^{ee} \delta \bar{\boldsymbol{\varepsilon}}_{eq,i} = f_{i-1}^e - \mathbf{K}_{i-1}^{ee} \bar{\boldsymbol{\varepsilon}}_{eq,i-1} \quad (2.2.42)$$

With

$$\mathbf{K}_{i-1}^{ee} = - \int_{\Omega} \mathbf{N}^e \mathbf{B} d\Omega \quad (2.2.43)$$

Combination of equation (2.2.38) and (2.2.42) results in a square system of equations,

$$\begin{bmatrix} \mathbf{K}_{i-1}^{uu} & \mathbf{K}_{i-1}^{ue} \\ \mathbf{K}_{i-1}^{eu} & \mathbf{K}_{i-1}^{ee} \end{bmatrix} \begin{bmatrix} \delta u_i \\ \delta \bar{\boldsymbol{\varepsilon}}_{eq,i} \end{bmatrix} = \begin{bmatrix} f_{ext}^u \\ f_{i-1}^e \end{bmatrix} - \begin{bmatrix} f_{int,i-1}^u \\ \mathbf{K}_{i-1}^{ee} \bar{\boldsymbol{\varepsilon}}_{eq,i-1} \end{bmatrix} \quad (2.2.44)$$

These coupled systems of equations are solved until convergence is reached.

## 2.3 Computation of damage using level set approach

In the local damage model the free energy per unit volume  $\varphi$  in the system depends on the strain  $\boldsymbol{\varepsilon}$  and a scalar damage variable  $D$

$$\varphi = \varphi(\boldsymbol{\varepsilon}, D) = \frac{1}{2}(1-D)\boldsymbol{\varepsilon} : \mathbf{E} : \boldsymbol{\varepsilon} \quad (2.3.1)$$

The state laws for stress  $\boldsymbol{\sigma}$  and the local energy release rate  $Y$  is obtained by differentiating the free energy

$$\boldsymbol{\sigma} = \frac{\partial \varphi}{\partial \boldsymbol{\varepsilon}} = (1-D)\mathbf{E} : \boldsymbol{\varepsilon} \quad (2.3.2)$$

$$Y = -\frac{\partial \varphi}{\partial D} = \frac{1}{2}\boldsymbol{\varepsilon} : \mathbf{E} : \boldsymbol{\varepsilon} \quad (2.3.3)$$

The evolution of damage is given by dissipation potential  $\chi^*(Y)$  [12]

$$\dot{D} = \frac{\partial \chi^*(Y)}{\partial Y}, Y = \frac{\partial \chi(\dot{D})}{\partial \dot{D}} \quad (2.3.4)$$

The above potentials  $\chi^*(Y)$  and  $\chi(\dot{D})$  are related by Legendre-Fenchel transformation

$$\chi(\dot{D}) = \sup_Y (Y\dot{D} - \chi^*(Y)), \quad \chi^*(Y) = \sup_{\dot{D}} (Y\dot{D} - \chi(\dot{D})) \quad (2.3.5)$$

From the above the damage evolution law is obtained as

$$\chi^*(Y) + \chi(\dot{D}) - Y\dot{D} \geq 0 \quad (2.3.6)$$

In the level set approach the level set  $\phi = 0$  is use to separate undamaged zone form the damaged one as shown in the Fig.2 [13]. The damage evolves over a length  $l_c$  leaving the completely damaged zone behind and is defined as an explicit function of level set as shown in Fig.3.

$$D = D(\phi), \quad D'(\phi) \geq 0 \quad (2.3.7)$$

Considering a domain  $\Omega$ , with some loading  $T$  applied on the part  $\Gamma_t$  and some displacement  $\mathbf{u}^*$  applied on the boundary  $\Gamma_u$ . Some part of  $\Omega$  may be completely damaged i.e.  $D=1$  and it is denoted by  $\Omega(\phi \geq l_c)$ .

The part of  $\Omega$  not fully damaged is given by

$$\Omega(\phi \leq l_c) = \{x \in \Omega : \phi(x) \leq l_c\} \quad (2.3.8)$$

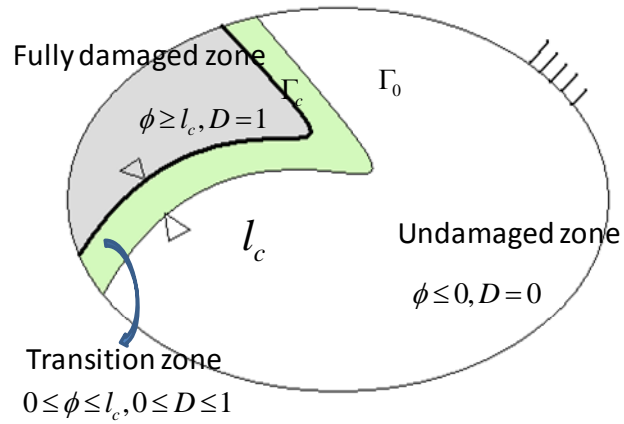


Figure2. Shows the level set method of separating the damaged and the undamaged zone along with the transition zone.

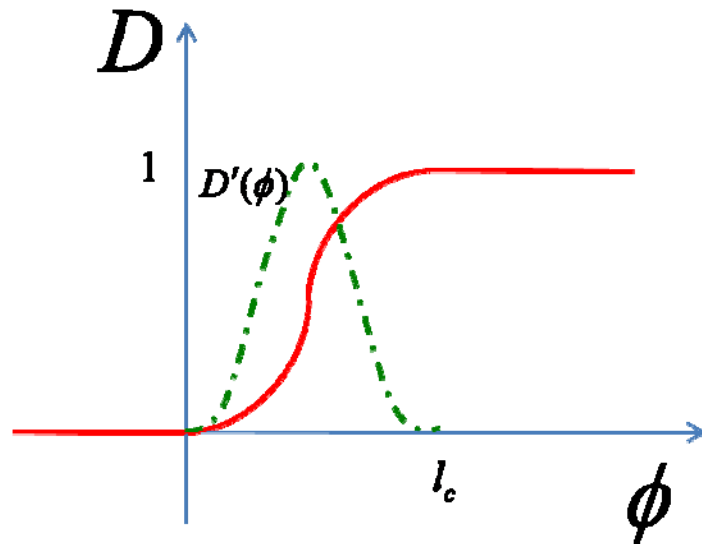


Figure3. Describes the damage function defined with respect to level set and its derivative.

The potential energy is expressed as a function of displacement field and the level set function

$$E(\mathbf{u}, \phi) = \int_{\Omega(\phi \leq l_c)} \chi(\boldsymbol{\varepsilon}(\mathbf{u}), D(\phi)) d\Omega - \int_{\Gamma_T} \mathbf{T} \cdot \mathbf{u} d\Gamma \quad (2.3.9)$$

Where  $\boldsymbol{\varepsilon}(\mathbf{u})$  denotes the symmetric gradient of  $\mathbf{u}$ .

The displacement field must satisfy the kinematic conditions and the gradient of level set must be of norm 1 (since it is a signed distance function). Thus the admissible displacement field is written as

$$A^d = \{(\mathbf{u}, \phi) : \mathbf{u} \in A_d^u, \phi \in A_d^\phi\} \quad (2.3.10)$$

$$A_d^u = \{\mathbf{u} : \mathbf{u} = \mathbf{u}^*, \Gamma_u\} \quad (2.3.11)$$

$$A_d^\phi = \{\phi : \|\nabla \phi\| = 1, \Omega\} \quad (2.3.12)$$

The admissible variation is thus defined as

$$A_0 = \{(\delta \mathbf{u}, \delta \phi) : \delta \mathbf{u} \in A_d^u, \delta \phi \in A_d^\phi\} \quad (2.3.13)$$

$$A_0^u = \{\delta \mathbf{u} : \delta \mathbf{u} = \mathbf{u}^*, \Gamma_u\} \quad (2.3.14)$$

$$A_0^\phi = \{\delta \phi : \nabla \delta \phi \cdot \nabla \phi = 0, \Omega\} \quad (2.3.15)$$

The condition on  $\delta \phi$  indicates that the variation of level set is constant along the normal path to the level set. This (2.3.15) condition implies that we chose  $\delta a(s)$  as the small perturbation along the damage front  $\Gamma_0$ .

$$\Rightarrow \delta \phi = \delta \phi(s) = \delta a(s) \quad (2.3.16)$$

In the curvilinear system of co-ordinates the  $(\phi, s)$  is expressed as

$$d\Omega = \frac{\rho(\phi, s)}{\rho(0, s)} d\phi ds \quad (2.3.17)$$

Where  $\rho(\phi, s)$  is the radius of curvature at  $(\phi, s)$  of the iso  $\phi$  curve.

The directional derivative of the potential energy is now computed with respect to  $(\delta \mathbf{u}, \delta \phi) \in A_d^0$  and by taking to account of the state laws (2.3.2) and (2.3.3)

$$DE(u, \phi)[(\delta u, \delta \phi)] = \int_{\Omega(\phi \leq l_c)} \boldsymbol{\sigma} : \boldsymbol{\varepsilon}(\delta u) d\Omega - \int_{\Gamma_T} T \cdot \delta u d\Gamma - \int_{\Omega(\phi \leq l_c)} Y D'(\phi) \delta \phi d\Omega \quad (2.3.18)$$

The equilibrium equation is obtained by zeroing the directional derivative of potential energy with respect to  $(\delta \mathbf{u}, 0) \in A_d^0$

$$DE(\mathbf{u}, \phi)[(\delta \mathbf{u}, 0)] = \int_{\Omega(\phi \leq l_c)} \boldsymbol{\sigma} : \boldsymbol{\varepsilon}(\delta \mathbf{u}) d\Omega - \int_{\Gamma_T} T \cdot \delta \mathbf{u} d\Gamma = 0 \quad \forall \delta \mathbf{u} \in A_d^0 \quad (2.3.19)$$

$D'(\phi)$  is non zero only in between 0 and  $l_c$  of the level set. This thick band is denoted as  $\Omega_{oc}$

$$\Omega_{oc} = \{x \in \Omega : 0 \leq \phi(x) \leq l_c\} \quad (2.3.20)$$

The variation of potential energy with respect to  $\phi$  is

$$DE(u, \phi)[(0, \delta \phi)] = - \int_{\Omega_{oc}} Y D'(\phi) \delta \phi d\Omega \quad (2.3.21)$$

$$= - \int_{\Gamma_0} \int_0^l Y(\phi, s) D'(\phi) \delta a(s) \frac{\rho(\phi, s)}{\rho(0, s)} d\phi d\Omega \quad (2.3.22)$$

$$= - \int_{\Gamma_0} g(s) \delta a(s) d\Gamma \quad (2.3.23)$$

This relation links the local damage variables  $Y$  and  $D$  to the homogenised one, the configurational force  $g(s)$  and the band location  $a$ .

The configurational force  $g(s)$  per unit length on the damage front is defined as

$$g(s) = \int_0^l Y(\phi, s) D'(\phi) \frac{\rho(\phi, s)}{\rho(0, s)} d\phi \quad (2.3.24)$$



Configurational force at a given point  $A$  along the damage front is given as

$$g(A) = \int_{AB} YD'(\phi) \frac{\rho(\phi)}{\rho(A)} d\phi \quad (2.3.25)$$

It gives the loss of energy as the front advances by a perturbation  $\delta a$ .

The dissipation in the system is given by the change in potential energy with respect to time

$$-\frac{dE(u, \phi)}{dt} = \int_{\Omega_{oc}} Y\dot{D}d\Omega = \int_{\Gamma_o} g\dot{a}d\Gamma \quad (2.3.26)$$

The evolution of damage is

$$\dot{D} = D'(\phi)\dot{a} \quad (2.3.27)$$

Given a field of  $Y$ , we must minimise the expression below

$$\inf_{\substack{\dot{D}=D'(\phi)\dot{a} \\ \Omega(\phi \leq l_c)}} \int \chi^*(Y) + \chi(\dot{D}) - Y\dot{D}d\Omega = \inf_{\dot{a}} \int_{\Omega(\phi \leq l_c)} \chi^*(Y) + \chi(D'(\phi)\dot{a}) - YD'(\phi)\dot{a}d\Omega \quad (2.3.28)$$

This minimization homogenises the evolution law over the band thickness. Since  $\dot{a}$  intervenes only in the last two terms the infimum reads as

$$\inf_{\dot{a}} \int_{\Omega(\phi \leq l_c)} \chi(D'(\phi)\dot{a}) - YD'(\phi)\dot{a}d\Omega \quad (2.3.29)$$

Integration above can also be limited to  $\Omega_{oc}$ . It can also be written as

$$\int_{\Omega(\phi \leq l_c)} YD'(\phi)\dot{a}d\Omega = \int_{\Gamma_o} g\dot{a}d\Gamma \quad (2.3.30)$$

The homogenised potential  $\bar{\chi}$  is defined as

$$\int_{\Gamma_o} \bar{\chi}(\dot{a}, s)d\Gamma = \int_{\Omega_{oc}} \chi(D'(\phi)\dot{a})d\Omega \quad (2.3.31)$$

and it depends explicitly on the location of the damage front. Now the infimum reads

$$\inf_{\dot{a}} \int_{\Gamma_o} \bar{\chi}(\dot{a}, s) - g \dot{a} d\Gamma = \sup_{\dot{a}} \int_{\Gamma_o} g \dot{a} - \bar{\chi}(\dot{a}, s) d\Gamma = \int_{\Gamma_o} \bar{\chi}^*(g, s) d\Gamma \quad (2.3.32)$$

The dual non-local potential  $\bar{\chi}^*$  is obtained through Legendre-Fenchel transformation. The non-local evolution law for the level set approach is written as

$$\dot{a}(s) = \frac{\partial \bar{\chi}^*(g(s), s)}{\partial g}, \quad \Leftrightarrow g = \frac{\partial \bar{\chi}(\dot{a}, s)}{\partial \dot{a}}, \quad \Leftrightarrow \bar{\chi}^*(g, s) + \bar{\chi}(\dot{a}, s) - g \dot{a} = 0 \quad (2.3.33)$$

Considering the damage evolution relation as shown below

$$\dot{D} = k \langle Y - Y_c \rangle_+^n = \frac{\partial \chi^*(Y)}{\partial Y} \quad (2.3.34)$$

Where  $Y_c$  is the critical energy release for the material above which the damage starts evolving, k and n are the positive constants.

The corresponding local damage potentials are obtained as shown below

$$\chi^*(Y) = \frac{k}{n+1} \langle Y - Y_c \rangle_+^{n+1} \quad (2.3.35)$$

$$\chi(\dot{d}) = \sup_Y (Y \dot{D} - \frac{k}{n+1} \langle Y - Y_c \rangle_+^{n+1}) \quad (2.3.36)$$

$$= Y_c \dot{D} + \left( \frac{1}{k} \right)^{m'} \frac{\dot{d}^{m'+1}}{m'+1} \quad (2.3.37)$$

$$\left| m' = \frac{1}{n} \right.$$

The configurational force for the given damage evolution reads as

$$g = \int_{AB} \left( Y_c + \left( \frac{1}{k} \right)^{m'} (D'(\varphi) \dot{a})^{m'} \right) D'(\varphi) dx \quad (2.3.38)$$

By considering a linear damage function  $d'(\varphi) = \frac{1}{l_c}$  as shown in the Fig.4 the

average energy release rate  $\bar{Y}$  and configurational force are obtained as

$$g = Y_c \frac{l}{l_c} + \left( \frac{1}{k} \right)^{m'} l \left( \frac{\dot{a}}{l_c} \right)^{m'} \quad (2.3.39)$$

$$\Rightarrow \bar{Y} = Y_c + \left(\frac{1}{k}\right)^{m'} l_c \left(\frac{\dot{a}}{l_c}\right)^{m'} \quad (2.3.40)$$

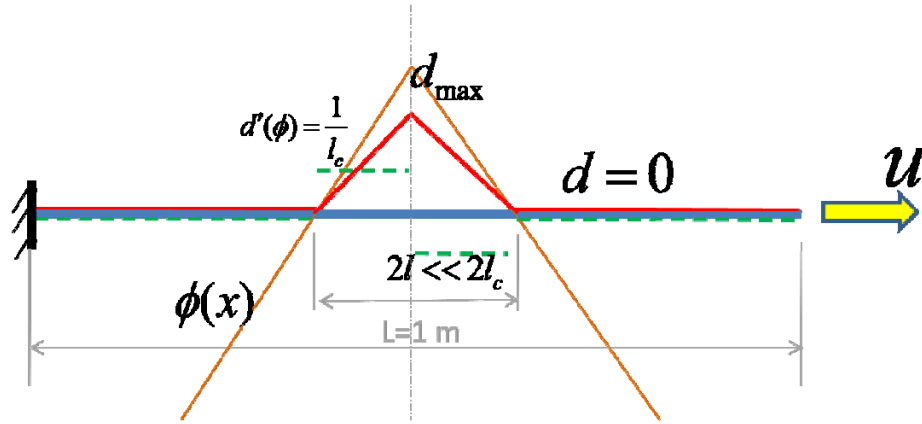


Figure4. Describe the level set representation of 1-D bar with the linear damage function.

### 3.0 MODELING PARAMETERS

The material models were analyzed using a 1D bar. The mesh sensitivity of the model is studied by varying the number of elements along the bar and the influences of various modeling parameters of the models were analyzed.

#### 3.1 Johnson Cook Visco-plasticity

The material constants of AISI 316L steel is used to study the Visco-plasticity model [7]. The value of the constants used for the study is shown in the Table. 1

The localization in the bar is caused by varying the temperature along the length of the bar. The lower temperature of 360 K is applied along the length of the bar ( $L = 1 \text{ m}$ ) and the 5% of the bar length in the middle is subjected to a higher temperature of 390 K. The velocity of the imposed displacement is taken as 8 m/s. It is imposed by taking the time step size of 0.01 s.

Material Constant	Value
yield strength of the material (A)	175 Mpa
Hardening modulus of the material (B)	380 Mpa
strain rate sensitivity coefficient (C)	1.0
Hardening coefficient (n)	0.32
Thermal coefficient (m)	1.0
Transition temperature, $T_m$	300 K
Melting temperature, $T_i$	1200 K
Density of the material, $\rho_h$	7850 Kg/m <sup>3</sup>
Heat capacity of the material, $C_p$	740 J/Kg/K
Youngs Modulus	290 Mpa

Table1. Values of constants used for Visco-plastic Model.

### 3.2 Gradient damage Model

The gradient damage approach is analyzed in a 1D bar with varying cross section as shown in the figure. The cross section of the bar is defined using the function (3.2.1) which is independent of the mesh number.

$$Area = Area * \left( 1 - \alpha * \exp \left( - \left( \frac{(x - x_c)}{L_c} \right)^2 \right) \right) \quad (3.2.1)$$

Where the amplitude of singularity is  $\alpha$ ,  $x$  is the distance in the bar,  $x_c$  location of the perturbation,  $L_c$  is the characteristic length for the variation of cross section.

For the present study  $x_c$  is located at the center of the bar and  $L_c$  is taken as 5% of the bar length i.e. 10% of the cross section is varied and  $\alpha$  is taken as 0.1.

The parameter which limits the localisation  $c$  is taken as 5. For the analysis the parabolic damage loading function (2.2.8) is taken into account with  $\varepsilon_{cr} = 2.10^{-4}$

The value of Youngs Modulus is taken as  $E = 15000Mpa$  and the length of the bar  $L=100$  m.

Linear interpolation is used for the average non-local strain equivalent equation and quadratic interpolation is used for the displacement as suggested in [11]. Usage of different interpolation function is not going to cause any influence on the computation, hence the choice is made for computational advantage. The bar is subjected to loading until failure. The Mesh sensitivity of the model is analyzed by varying the number of elements along the bar and the influence of parameter  $c$  is studied on its effect on strain localisation.

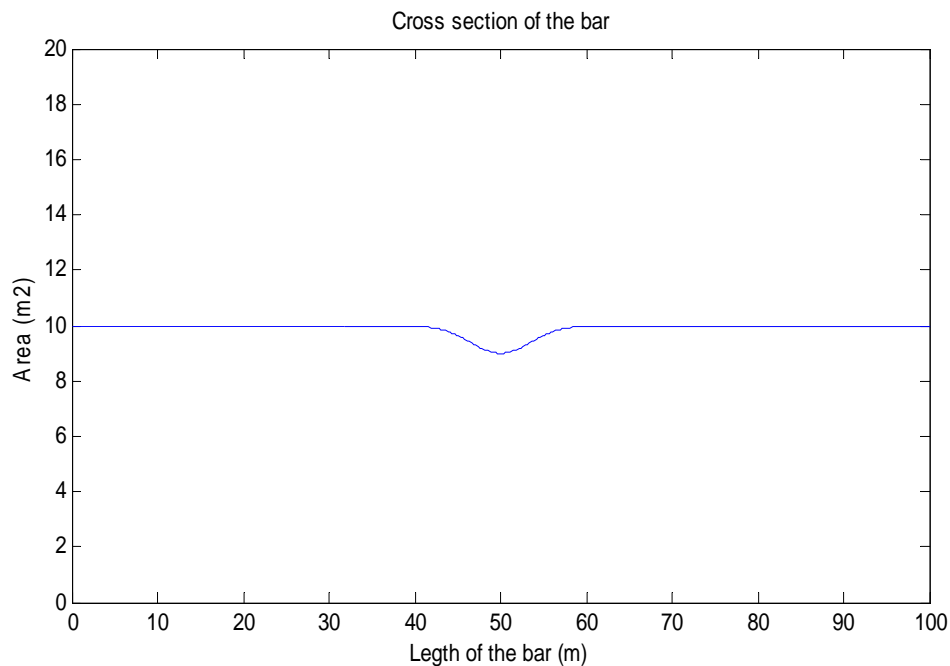


Figure5. Show the area distribution with respect to the bar length in non-local gradient model.

### 3.3 Level set approach

In the level set approach the three different damage function is analysed. Linear damage function where the damage grows linearly with respect to the distance along the normal path of the level set as shown below

$$D = \frac{l}{l_c} \quad (3.3.1)$$

Second damage function used similar to the one applied in solidification of solids is studied(3.3.2). Where  $\gamma = \frac{l}{l_c}$

$$D = 4\gamma^3 - 3\gamma^4 \quad (3.3.2)$$

And the third damage function where  $\left(\frac{1}{1-D}\right)$  is linear is taken in to account

$$D = 1 - \left(\frac{l_c}{l + l_c}\right) \quad (3.3.3)$$

Figure 6 shows the plot of damage functions with respect to the length of damage. The damage function reaches their maximum at a distance  $l_c$ .

And three different damage evolution laws were considered as shown below

$$\bar{Y} = Y_c \quad (3.3.4)$$

Here the average non-local equivalent energy release is equated to the critical energy release rate specified for the material.

A hardening type damage evolution is considered as show below

$$\bar{Y} = Y_c + \mu Y_c \quad (3.3.5)$$

Where  $\mu$  is positive growing function linked to the damage of the material. For the present study it is taken as equal to the damage D.

The Visco plastic damage growth model is studied as shown below

$$\dot{D} = k \langle \bar{Y} - Y_c \rangle_+^n \quad (3.3.6)$$

Where  $k$  and  $n$  are positive constant. The value of Length of the bar ( $L=500$  m), Youngs Modulus  $E=500$  Mpa, and the Critical Energy release ( $Y_c=1e-3$ ) are chosen such that the maximum force and displacement in the bar is unity.

The bar is subjected to loading until the damage reaches the maximum limit i.e.  $l_c$ . The length of the damage function to reach the maximum value ( $D=1$ ).

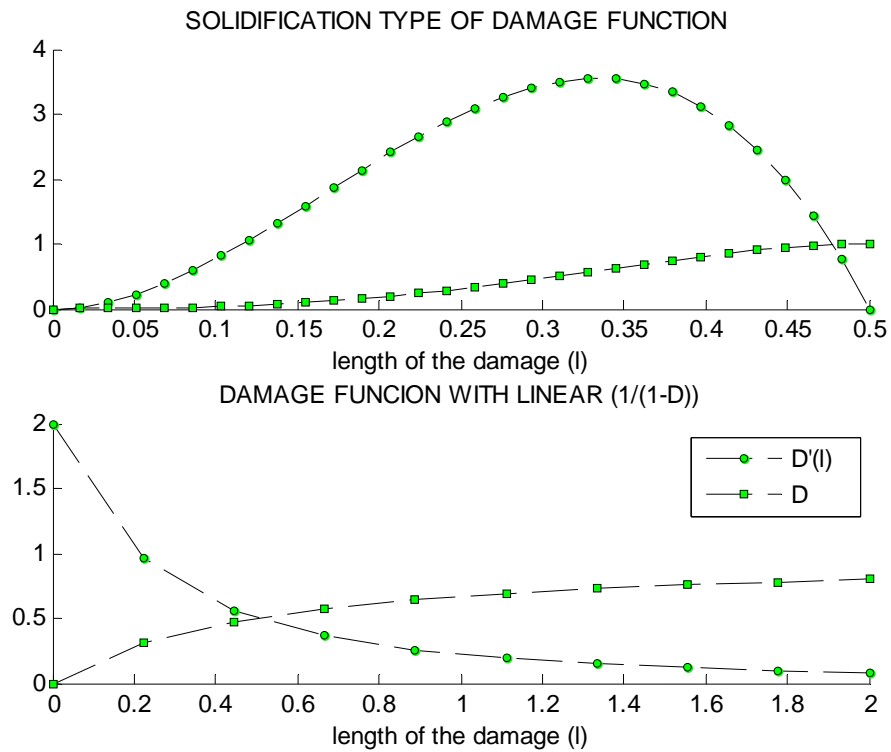


Figure6. Show the damage and its derivative functions used in level set approach with respect to their length of damage

## 4.0 RESULTS AND DISCUSSION

### 4.1 Johnson Cook Visco-plasticity

Figure7. Show the total strain along the length of the bar after each increment to imposed displacement for the Johnson cook Visco-plasticity Model. Form the figure it's clear that the strain localises in a very sharp narrow region known as strain localization zone, where the variation in temperature is introduced in the bar.

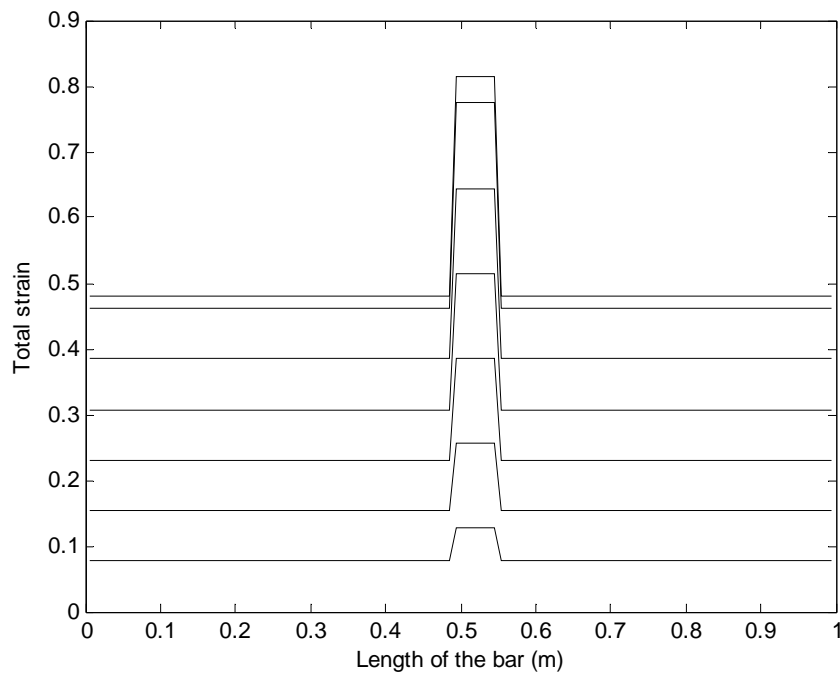


Figure7. Displacement at increment of imposed velocity along the length of the bar for visco-plastic regularisation model.



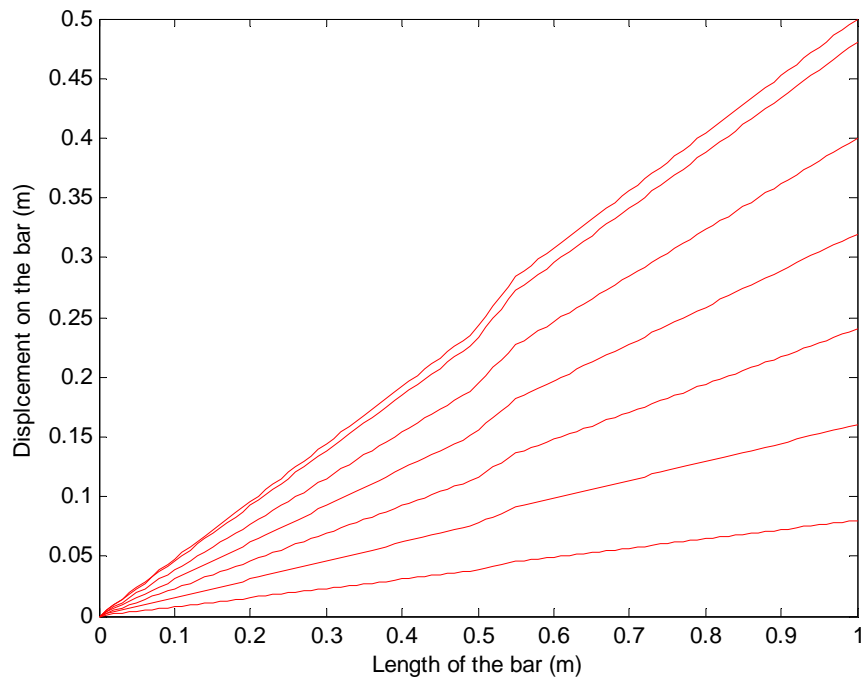


Figure8. Displacement at increment of imposed velocity along the length of the bar for visco-plastic regularisation model.

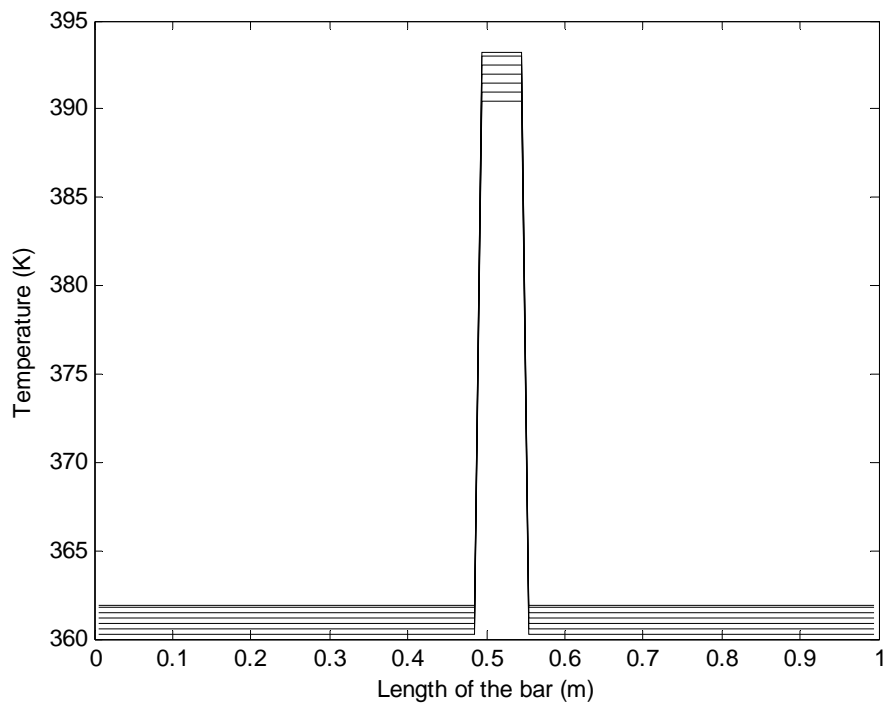


Figure9. Temperature distribution at increment of imposed velocity along the length of the bar for visco-plastic regularisation model.

Displacement along the length of the bar is shown in Fig. 8 after each increment of imposed displacement. Change in slope of displacement with respect to the length of the bar is observed in the localized zone. Fig. 9 Show the temperature distribution along the bar after each increment of imposed displacement. It shows the increment in temperature with respect to the loading and it is more significant in the zone of localization. The diffusion effect of temperature is not observed in the viscoplastic model.

### 4.2 Gradient damage Model

Figure10. Show the Evolution of damage along the length of the bar after each increment of imposed displacement. Thus the zone of strain localisation is obtained in the middle of the bar as expected where the cross sectional area is reduced. In the present study the value of damage is same as the average strain equivalent. The diffusion of strain is clearly visible from the figure. This diffusion effect and average of strain over a region helps to reduce the mesh sensitivity of the Material Model.

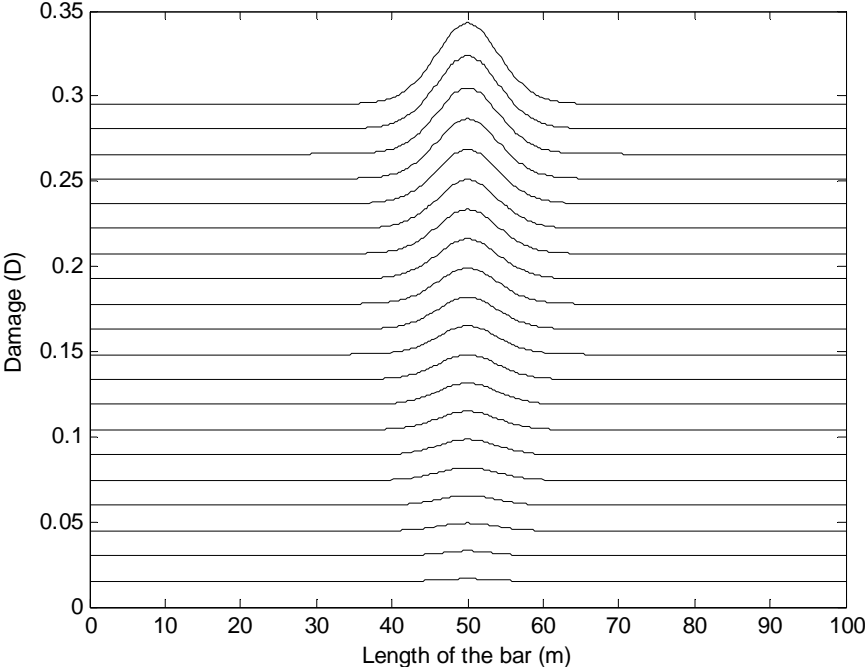


Figure10. Evolution of damage along the length of the bar after each increment of imposed displacement.

Mesh sensitivity of the model is analysed by varying the number of elements along the length of the bar. The model is very less sensitive to the variation above a certain number of elements. However the variation is observed for less number of elements in the bar. Fig. 11 shows the damage in the bar for Meshes with 5, 10 and 15 number of elements. In general mesh sizes to get minimum of three element in the localization zone is recommended for this model. It is worth to recal that quadratic interpolation is used for displacement in the present study.

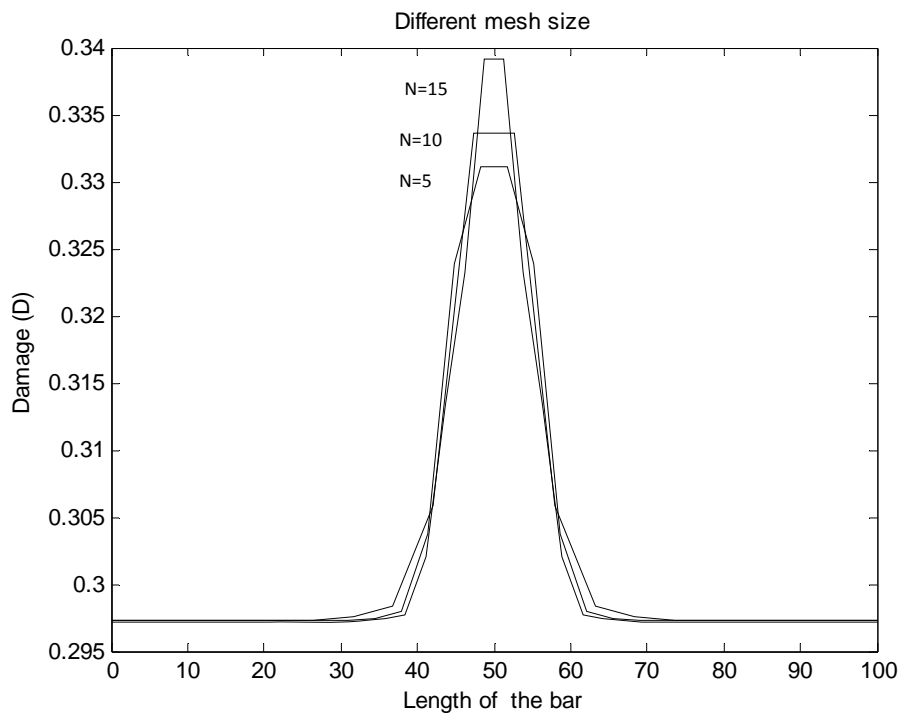


Figure11. Influence of mesh size on damage evolution along the length of the bar, Mesh sizes of 5, 10 and 15 elements were considered.

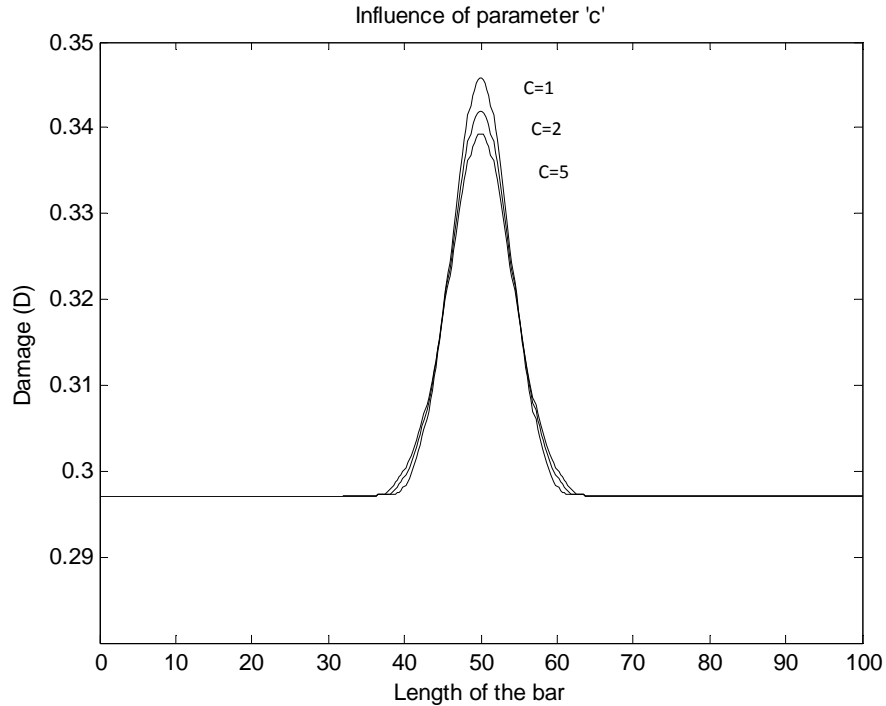


Figure12. Influence of parameter  $c$  on damage localisation, damage for values  $c=1, 2$  and  $5$  were plotted.

Influence of characteristic length parameter is studied by varying it to values 1, 2 and 5 in the present study. The damage in the bar for each of the values is shown in Fig. 12. It shows the effect of characteristic length in the diffusion of damage in the bar. The diffusion increases with increase in the value of ' $c$ '. This is due to increase in the domain of averaging space to compute strain equivalent of the model. In general the value of  $c$  is chosen based on the microstructural size of the material.

Stress-Strain plot for the non-local gradient damage model using parabolic damage evolution is shown in Fig. 13. From the numerical aspect the computation effort increases with the non linearity effect of the material. It is observed that the number of Newton iteration required for convergence increases as the slope of tangent of the stress-strain curve decreases. In order to obtain the full stress strain curve until fracture special algorithm such as Arc-length should be applied to the Newton solution procedure.

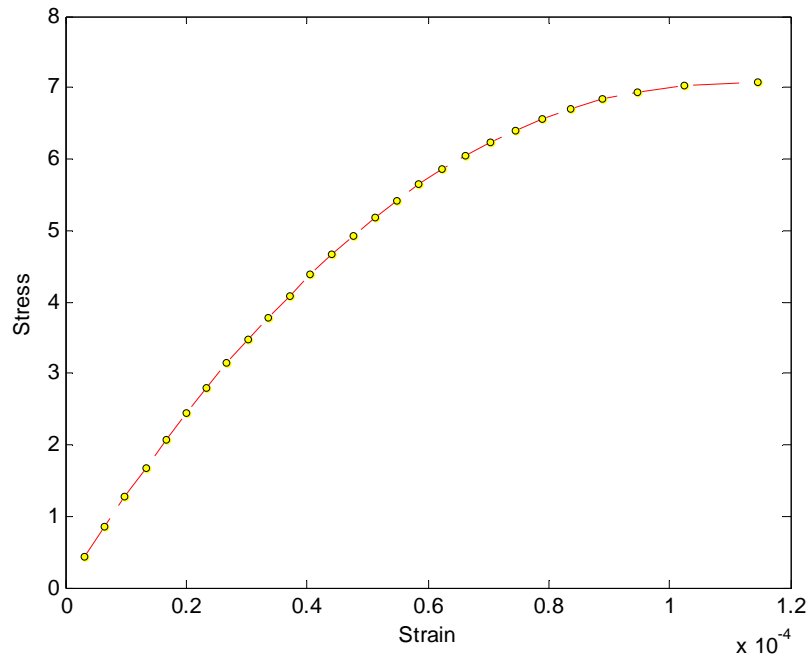


Figure13. Stress-Strain plot for the non-local gradient damage model using parabolic damage evolution.

### 4.3 Computation of damage using level set

#### 4.3.1 Analytical Solution

The analytical solution to the proposed level set approach is obtained as for a 1D bar of length  $L$  subjected to a imposed displacement of  $U$  as shown in the figure 14. The damage initiation is assumed to start from one end of the bar and it can grow and its extension is denoted as  $l$ . The damage in 1D can grow until failure i.e. to the distance of  $l_c$ .

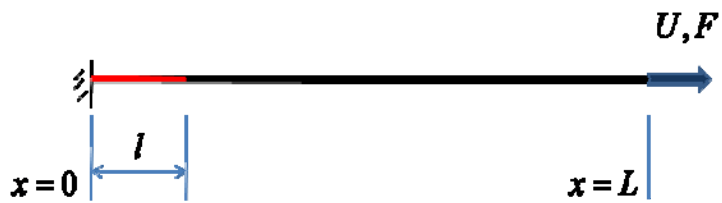


Figure14. A bar subjected to loading with the damage of length  $l$

Since the Force  $F$  along the length of the bar is uniform. The force displacement relationship is given by the compatibility condition as shown in (4.3.1)

$$\int_0^l \frac{F}{E(1-D)} dx + \int_l^L \frac{F}{E} dx = U \quad (4.3.1)$$

$$\Rightarrow \frac{F}{U} = E \left( \int_0^l \left( \frac{1}{1-D} \right) dx + (L-l) \right)^{-1} \quad (4.3.2)$$

By considering the linear damage function (3.3.1) and the damage evolution law (3.3.4) the displacement on the bar and the corresponding force is obtained.

$$\int_0^l YD'(\phi) dx = \bar{Y}_c \quad (4.3.3)$$

$$\int_0^l \frac{1}{2} E \varepsilon^2 \frac{1}{l_c} dx = Y_c \frac{l}{l_c} \quad (4.3.4)$$

$$\Rightarrow F = \text{SQRT} \frac{2EY_c l \left( 1 - \frac{l}{l_c} \right)}{\left( l_c - l_c \left( 1 - \frac{l}{l_c} \right) \right)} \quad (4.3.5)$$

The displacement in the bar is calculated by substituting the obtained force in the equation (4.3.1).

$$U = \frac{Fl}{E \left[ 1 - \left( \frac{l}{2l_c} \right) \right]} \quad (4.3.6)$$

#### 4.3.1.1 Influence of Damage evolution law

Influence of damage evolution law in the level set approach is analysed by applying the different damage evolution in the 1D bar and by using the linear damage function.

The analytical solutions for load Vs displacement using linear damage function and damage evolution law  $\langle Y \rangle = Y_c$  for different value of  $l_c$  is shown in Fig. 15. The elastic loading takes place until the maximum force is reached and then tangential return of the curve is observed as the damage grows. The damage grows and reaches the maximum limit  $l_c$  causing ultimate fracture. It is clear that the area between the elastic loading curve and the return curve increases with the increase in  $l_c$ . The material becomes more ductile and due to higher dissipation in the system. The tangential return at the initial unloading can be interpreted as the increase in damage without considerable dissipation in the system. The damage initiation takes place in the local sense and then the averaging space to compute the configurational force grows along with the damage zone.

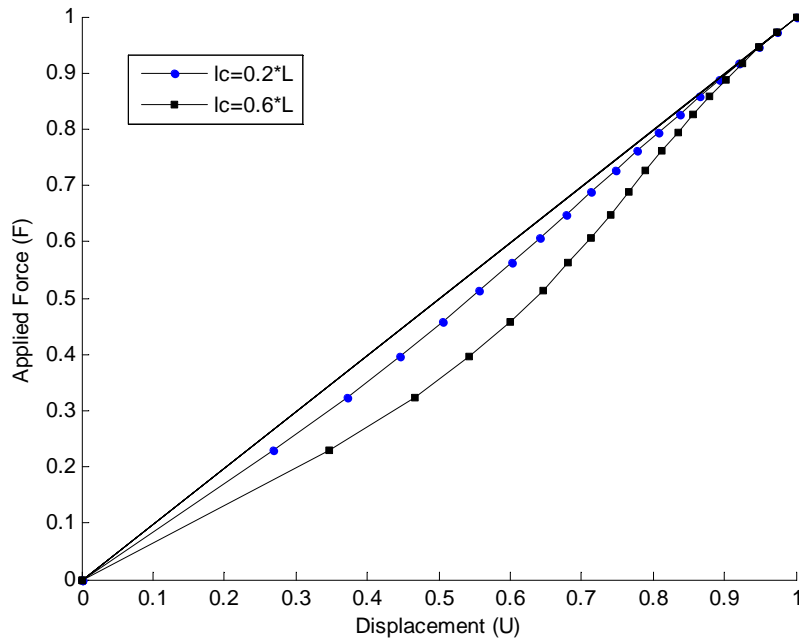


Figure15. Force Vs displacement plot for different  $l_c$  using linear damage function and evolution law  $\langle Y \rangle = Y_c$

Force Vs displacement plot for different  $l_c$  using linear damage function and Hardening type evolution law is shown in Fig.16. The tangential return during initial unloading is affected by using hardening type evolution law. Thus more energy is spent

during the initial damage growth process. Also the material becomes more ductile with increase in  $l_c$ .

Force Vs displacement plot for Visco plastic type evolution law for different imposed velocity is shown in Fig.17. In the viscoplastic law the constants are taken as  $k=2$  and  $n=2$ . With the increase in rate of deformation the maximum force required to initiate damage is increased. Also the tangential return of the returning curve is also affected by using the viscoplastic relation.

The material becomes in sensitive to rate effects i.e. tends to plastic when  $k \rightarrow \infty$  &  $n \rightarrow 0$  and they acts as the controlling parameter to the model (Fig.18). By increasing the length of damage the dissipation in the system is increased.

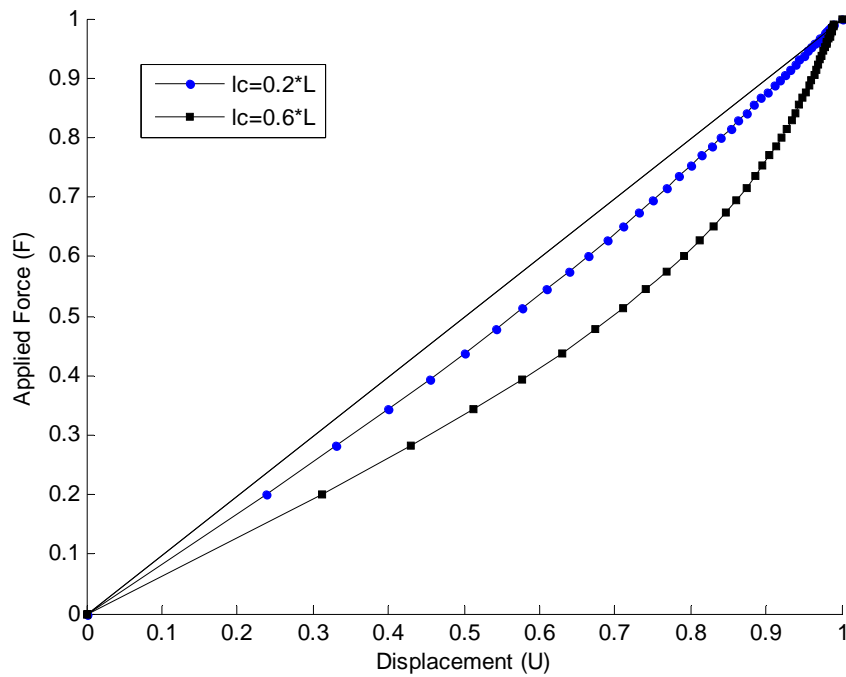


Figure16. Force Vs displacement plot for different  $l_c$  using linear damage function and Hardening type evolution law.



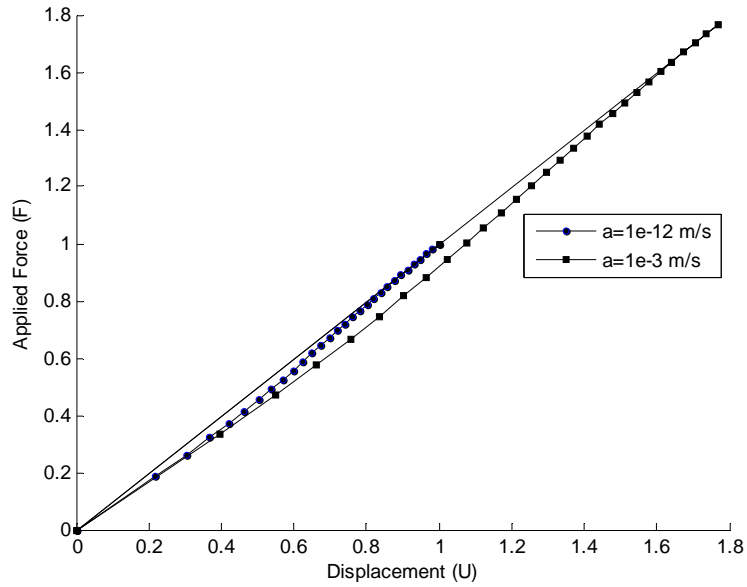


Figure17. Force Vs displacement plot for different  $l_c$  using linear damage function and viscoplastic type evolution law.

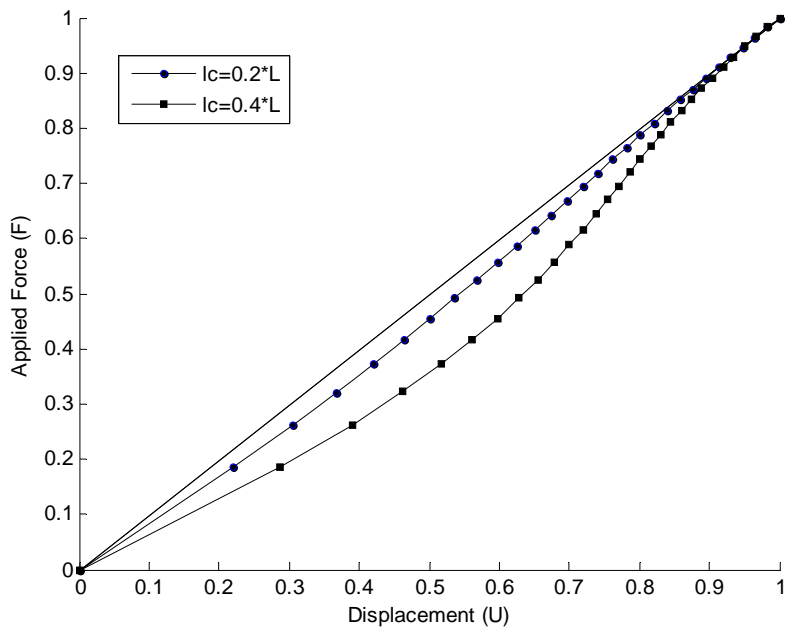


Figure18. Force Vs displacement plot for different  $l_c$  using linear damage function and viscoplastic type evolution law.

### 4.3.1.2 Influence of Damage function

Influence of damage evolution law in the level set approach is analysed by applying the different damage function in the 1D bar and by using the hardening type evolution law. Force Vs displacement plot using linear  $\left(\frac{1}{1-D}\right)$  damage function and hardening type evolution law is shown in Fig.19. Here the material flows after reaching the maximum elastic load and flows without offering any resistance.

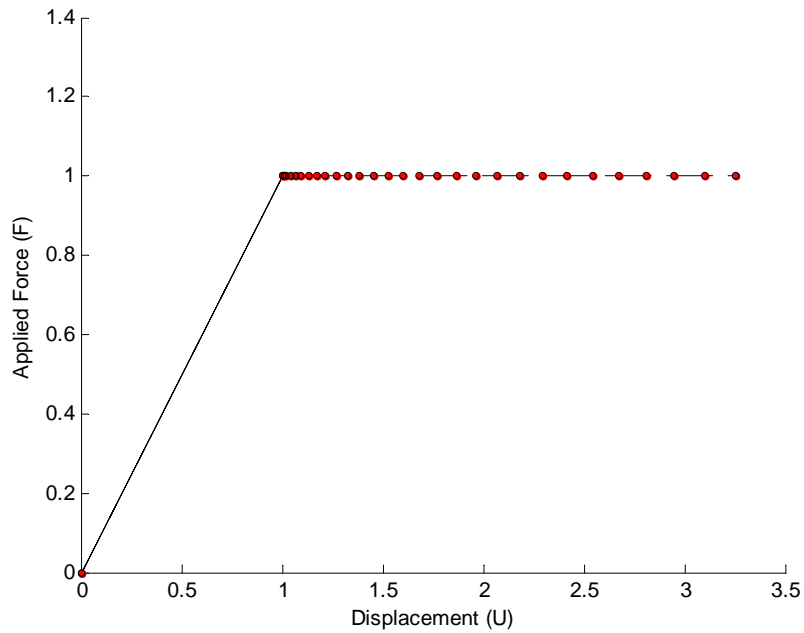


Figure19. Force Vs displacement plot using linear  $\left(\frac{1}{1-D}\right)$  damage function and hardening type evolution law.

Solidification type of damage function is used for the study and the Figure19. Force Vs displacement plot using the Solidification type damage function is shown in Fig. 20. The dissipation in the system increases with increase in  $l_c$ .

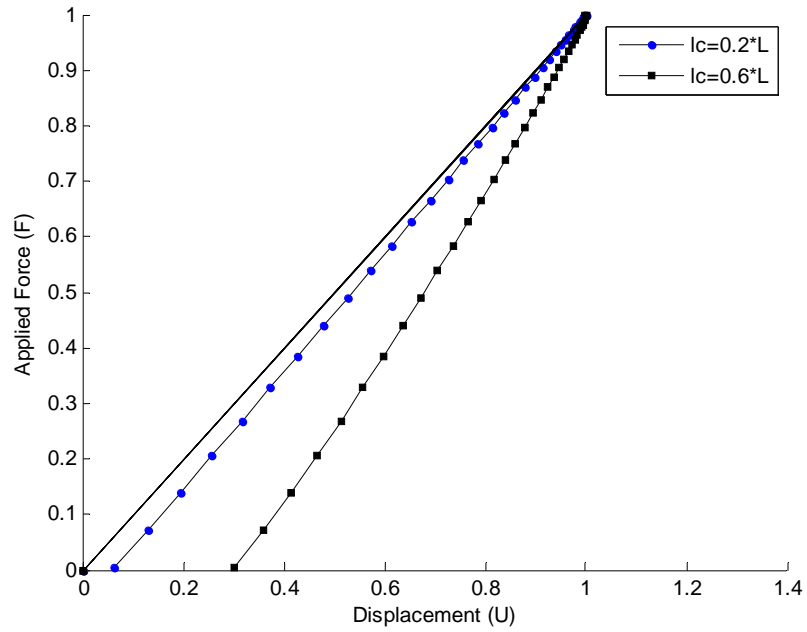


Figure20. Force Vs displacement plot for different  $l_c$  using solidification type damage function and hardening type evolution law.

### 4.3.2 Finite element Solution

A 1D is subjected to loading until failure. The bar is discretized using 1D linear elements, while N being the number of elements. The finite element computation of the level set approach is summarized below

Initialisation of material and Geometric constants

$$E, L, N, Y_c, l_c$$

Force  $F$  is applied; Local Energy release  $Y$  is computed along the Gauss Points

Check  $Y_{\max} \leq Y_c$

Update length of damage  $\delta$

Compute the Force in the bar  $F = f(l + \delta)$

Compute the new damage values along the gauss points

Compute the Displacement along the bar

Check  $l < l_c \quad F > 0$

End

Since the level set control over the element integration is not implemented in the present analysis, the length of damage update is equal to the element size as shown in the Fig.21. It is convincing that the level set incorporation leads to precise calculation of energy release irrespective of the mesh size, which make them mesh insensitive. The Force Vs displacement plot for Finite Element calculation using linear type damage function and evolution law  $\langle Y \rangle = Y_c$  is shown in Fig. 22.



Figure21. Shows the finite element Discretization of the bar for level set approach and the damage function growth.

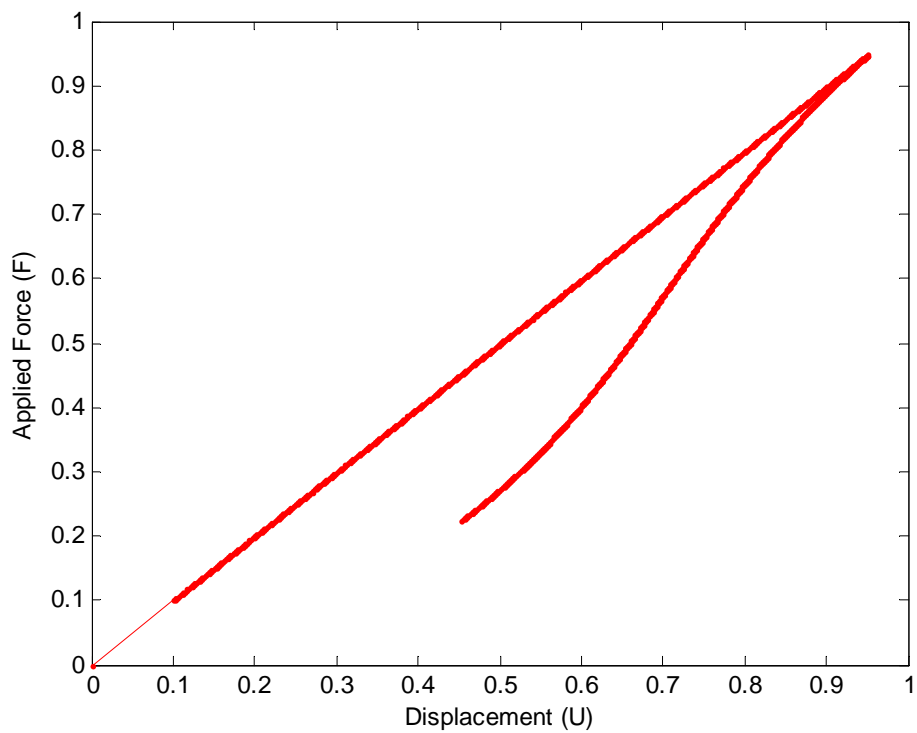


Figure22. Force Vs displacement plot for Finite Element calculation using linear type damage function and evolution law  $\langle Y \rangle = Y_c$

## 5.0 CONCLUSION

- The Johnson Cook Viscoplastic Model and Non-local gradient Model were analyzed for the 1D bar. A new level set approach is proposed as an effective alternative.
- In the Level set based approach, Level set is used to separate damage zone and the undamaged zone with the damage function interlinking them to form the transition zone.
- Non-locality is introduced by regularization of energy release in the transition zone and the configurational force required to propagate damage in the damage front is computed.
- Robustness of the proposed approach is demonstrated by applying different Damage functions and Damage evolution law to fit the desired material behavior.

### Advantages of the proposed approach

- Use of Level set gives greater control over the damage zone and could facilitate merging and branching of the damage zone.
- Transition from damage to fracture is well defined and the model permits the fully damaged zone in the material ( $D=1$ ).
- The non-local gradient type approach is computationally expensive than level set approach. In the non-local gradient approach the strain regularization is carried out for the entire domain where as in the level set approach the regularization is done only in the transition zone.
- The model is very less sensitive to mesh size due to non-locality introduced by homogenization.

## 6.0 REFERENCE

1. W. Xue-bin, Temperature distribution in adiabatic shear band for ductile metal based on Johnson-Cook and gradient plasticity models, *Trans. Nonferrous Met. Soc. China*, Vol. 16, pp. 333-338, 2006.
2. C.K.Syn, D.R.Lesuer and O.D.Sherby, Microstructure in adiabatic shear bands in a pearlitic ultrahigh carbon steel, UCRL, JRNL, 200196.
3. W. Xue-bin, Analysis of Damage localization for ductile metal in process of shear band propagation, *Trans. Nonferrous Met. Soc. China*, Vol. 16, pp. 153-158, 2006.
4. J.W.Rudnicki and J.R.Rice, Conditions for the localization of deformation in pressure-sensitive dilatant materials, *J.Mech.Phys.Solids*, Vol.23, pp. 371-394.
5. J.Zhao, D.Sheng and W. Zhou, Shear banding analysis of geomaterials by strain gradient enhanced damage model, *International Journal of Solids and Structures*, Vol. 42, pp. 5335–5355, 2005.
6. J.H.P.Vree, W.A.M.Brekelmans and M.A.J.Van Gils, Comparison of non-local approaches in continuum damage mechanics, *Computers & Structures*, Vol.55, No.4, pp. 581-588, 1995.
7. D.Umbrello, R.M.Saoubi and J.C.Outeiro, The influence of Johnson-Cook material constants on finite element simulation of AISI 316L steel, *International Journal of Machine Tools & Manufacture*, Vol. 47, pp. 462-470, 2007.
8. Z.P. Bazant and B. Oh, Crack Band theory for fracture of concrete, *RILEM materials structures*, Vol. 16, pp. 155–177, 1983.
9. J.Mazars and Pijaudier–cabot, Continuum damage theory – application to concrete, *Journal of Engineering Mechanics*, ASCE, Vol. 115, pp. 345–365, 1989.
10. R.H.J. Peerlings, R.de Borst, W.A.M. Brekelmans and J.H.P. de Vree, Gradient-enhanced damage for quasi-brittle materials, *International Journal for Numerical Methods in engineering*, Vol. 39(19), pp. 3391 – 3403, 1998.

11. R.H.J. Peerlings, R.de Borst, W.A.M.Brekelmans and J.H.P.de Vree, Computational Modelling of Gradient-enhanced damage for fracture and fatigue problems, Internal report Delft University of Technology, WFW 94.132, 1994.
12. J. Lemaitre, J.L. Chaoche, Mechanics of Solid Materials, Cambridge University press, Cambridge, 1990.
13. N. Moës, C.Stolz, N.Chevaugeron and P.E. Bernard, A new level set based regularization technique for local damage model, Internal Report, Ecole centrale de Nantes, 2009.